Progress In Electromagnetics Research B, Vol. 86, 121–138, 2020

High Q-Factor Bandstop Filter Based on CPW Resonator Broadside-Coupled to CPW Through-Line

Walid M. Fahmy[1], Asmaa E. Farahat[1], Khalid F. A. Hussein[1, *], and Abd-El-Hadi A. Ammar[2]

Abstract—High Q-factor bandstop filter based on broadside-coupling between U-shaped coplanar waveguide (CPW) resonator and CPW through-line (CPWTL) is proposed in the present paper. The CPWTL is printed on the top layer of the dielectric substrate whereas the CPW resonator (CPWR) is printed on the bottom layer. Only over very narrow frequency band around the resonant frequency of the CPWR the microwave power flowing in the CPWTL is coupled to (absorbed by) the CPWR leading to a bandstop filter of very high Q-factor. A CPWR with side ground strips of finite width is shown to have much higher Q-factor than that of infinitely extending side ground planes. Owing to the lower profile of the CPW with finite-width, the radiation loss is reduced, and the structure has narrower frequency band for coupling, which results in much higher Q-factor than other published works. The dimensions of the CPWTL are optimized for impedance matching whereas the dimensions of the U-shaped CPWR are optimized to obtain the highest possible Q-factor. The effect of the loss tangent of the dielectric substrate material on the Q-factor is investigated. A prototype of the proposed filter is fabricated and experimentally studied for more understanding of the underlying physical principles of operation and for experimental investigation of the filter performance. The experimental measurements show good agreement with the corresponding simulation results.

1. INTRODUCTION

Microwave fields in three-dimensional [1, 2], two-dimensional (printed patches or etched slots), and quasi-one dimensional cavities (printed transmission lines) [3, 4] are known to exhibit very sharp peaks over very narrow frequency intervals leading to very high Q-factor resonators. Such resonators can be used to design high Q-factor bandpass and bandstop filters. Microwave high Q-factor bandstop filters have been widely used in communication systems for rejecting unwanted frequency signals to enhance the system performance [5–8]. For example, in satellite communication systems, particularly in the transceiver of the ground station, the bandstop filters are often needed in the frond-end to pass the downlink signals received by the ground station antenna and to block the uplink signals originated at the transmitting antenna of the same ground station. An analogous role is played by the bandstop filter of the satellite transceiver. Multiple-band bandstop filters are required for many applications [9–15].

A coplanar waveguide (CPW) has the principal advantage that the signal line and signal grounds are placed on the same substrate surface. This eliminates the need for via holes and, thereby, simplifies the circuit fabrication. Moreover, this allows simple connection of series as well as shunt components [16–18]. Another major advantage of CPW is that it exhibits lower conductor loss than microstrip lines [19, 20]. Also, circuit design can be based on both the odd and even CPW modes [21]. Moreover, CPWs are

Received 23 December 2019, Accepted 8 February 2020, Scheduled 20 February 2020

* Corresponding author: Khalid F. A. Hussein (khalid_elgabaly@yahoo.com).

[1] Microwave Engineering Department, Electronics Research Institute, Cairo, Egypt. [2] Electronics and Electrical Communications Department, Faculty of Engineering, Al-Azhar University, Cairo, Egypt.

open structures and do not require metallic enclosures [21]. CPW resonators have their distributed element construction avoiding uncontrolled stray inductances and capacitances, and, thereby, have better microwave properties than lumped element resonators [3].

Improvement of the Q-factor of bandstop filters has been achieved in literature using printed transmission lines with a defected ground structure (DGS) [22–25]. However, the achieved Q-factor is always limited to a few dozens or even lower with some complexity of the structure and needs for lumped elements. End-coupled and edge-coupled CPW resonator structures are commonly used for microwave and millimeter-wave filter designs [26]. In end-coupled resonators, the interchange of energy with the coupling gap may be insufficient, even when very narrow gaps are employed. Due to this reason parallel- or edge-coupled CPWRs are more commonly used than end-coupled CPWRs [26]. However, broadside coupling results in the strongest coupling among all these coupling methods [7]. For the bandstop filter proposed in the present work, the CPW structure has the advantage that it allows printing the CPWR on the bottom layer of the dielectric substrate and the CPW through-line (CPWTL) on the top layer, which enables enhanced broadside coupling. Owing to such a geometry, this structure has the advantage that the length over which the broadside coupling is achieved can be easily set to get the required bandwidth of the bandstop filter or, equivalently, the Q-factor. On the other hand, the center frequency can simply be tuned by setting the CPWR length to the corresponding value. Moreover, the input impedance of the CPWTL is not sensitive to the substrate thickness, which allows impedance matching independent of the substrate thickness. This provides the design freedom to use the substrate thickness as a major design parameter for controlling the strength of broadside coupling and, hence, the Q-factor of the bandstop filter.

A prototype of the proposed high Q-factor bandstop filter is fabricated and experimentally studied for more understanding of the underlying physical principles of operation and for verifying some of the simulation results.

2. THE PROPOSED BANDSTOP FILTER DESIGN

The proposed bandstop filter has the geometry shown in Figure 1 with the indicated symbolic dimensional parameters. This filter is constructed as a U-shaped CPWR broadside coupled to a CPWTL. Both the CPWR and CPWTL have finite width ground strips as shown in the figure. The U-shaped CPWR is an open-ended half-wavelength resonator. This design necessitates that the CPWR has the same cross section as that of the CPWTL, i.e., the strips and slots of the CPWR have the same width as those of the CPWTL. As long as the operating frequency is far from the resonant frequencies of the U-shaped CPWR, the CPWTL is almost unloaded leading to complete microwave power transfer between the filter ports (1) and (2). Only over very narrow frequency band around the resonant frequency, the microwave power is absorbed and stored in the U-shaped CPWR preventing any power transfer between the filter ports and, thereby, leading to high Q-factor bandstop filter response.

The finite width of the side ground strips of the CPWR results in much higher Q-factor than that obtained when using a CPWR of infinitely extending side ground planes. The lower profile of the CPW with finite-width ground results in lower radiation loss and narrower frequency band for coupling, which, in turn, enhances the Q-factor.

The most important design goals of the proposed bandstop filter are impedance matching at the filter ports, the required center frequency, and the required bandwidth (equivalently, the Q-factor). One of the major advantages of the proposed design is that each of these design goals can be achieved (almost independently of the other two goals) by adjusting only one or two independent dimensional parameters. The following table gives a list of the dimensional parameters that can be used to achieve the required filter performance metrics.

It should be noticed that each of the design dimensional parameters (s, w, L_R, L_B, h) can be set to significantly affect one of the design goal parameters (Z_{in}, f_{c}, Q) according to Table 1 without significant effects on the other design goal parameters. The design rules to achieve the bandstop filter design goals are discussed in detail in Section 3.

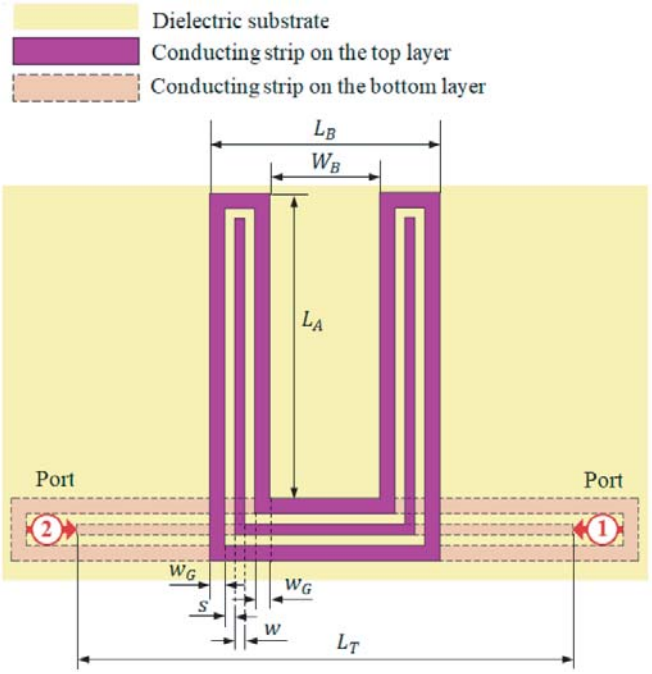

Figure 1. Schematic of the proposed design for high Q-factor bandstop filter constructed as CPWTL broadside-coupled to a U-shaped CPWR.

Table 1. List of the independent design parameters that can be used to achieve the design goals of the bandstop filter.

Design Goal		Dimensional Parameter	
Symbol	Description	Symbol	Description
Z_{in}	Input Impedance	s	Central Strip Width
		w	Side Slots Width
f_{c}	Center Frequency	L_R	Resonator Length
Q	Q-factor	L_B	Coupling Length
		h	Substrate Height

3. RULES FOR THE BANDSTOP FILTER DESIGN

The length L_R of an open-ended CPWR is inversely proportional to the resonance frequency which can be expressed as follows [27].

$$f_n = \frac{nc}{2L_R\sqrt{\varepsilon}_{r_{eff}}}, \quad n = 1, 2, \ldots \tag{1}$$

where c is the velocity of light in free space, n the resonance mode order, and $\varepsilon_{r_{eff}}$ the effective dielectric constant of the quasi-TEM mode of the CPW.

The effective dielectric constant of the quasi-TEM mode of the CPW can be expressed as follows [27].

$$\varepsilon_{r_{eff}} = 1 + \frac{\varepsilon_r - 1}{2} \frac{K\left(\acute{k}_0\right)}{K\left(k_0\right)} \frac{K\left(k_1\right)}{K\left(\acute{k}_1\right)} \tag{2}$$

where ε_r is the dielectric constant of the substrate material, and K denotes the complete elliptic integral

of the first kind, which is defined as follows.

$$K(k) = \int_0^{\frac{\pi}{2}} \frac{d\theta}{\sqrt{1 - k\sin^2\theta}} \tag{3}$$

The arguments, k_0, $\acute{k}_0$, k_1, and $\acute{k}_1$, of K are defined as follows.

$$k_0 = \frac{s}{s+2w},\ \acute{k}_0 = \sqrt{1-k_0^2},\ k_1 = \frac{\sinh(\pi s/4h)}{\sinh[\pi(s+2w)/4h]},\ \acute{k}_1 = \sqrt{1-k_1^2} \tag{4}$$

The characteristic impedance of the quasi-TEM mode of the CPW is expressed as follows [28].

$$Z_0 = \frac{30\pi}{\sqrt{\varepsilon}_{r_{eff}}} \frac{K\left(\acute{k}_0\right)}{K(k_0)} \tag{5}$$

In spite of being formulated for a CPW of infinitely extending ground, Equations (2) and (5) can be used as preliminary design rules for a CPW with side ground strips of finite width with good accuracy as long as $w_G > w$ and $w_G > s$.

According to Eq. (5), a $50\,\Omega$ characteristic impedance of the CPWTL can be obtained by setting the proper values of the strip and slot widths.

3.1. Calculating the Quality Factor of the Bandstop Filter

The broadside coupling between the U-shaped CPWR and the CPWTL causes external loading on the resonator. As a consequence, the resonance frequency can be shifted (from that of the unloaded resonator) because the reactive coupling as part of the energy is stored in the electric field of the coupling reactance. Besides, due to such reactive coupling, the resultant (loaded) quality factor (Q) is decreased as the broadside coupling to the through-line can be considered as a loss channel. Thus, the total (loaded) Q-factor can be evaluated through the following relation.

$$\frac{1}{Q} = \frac{1}{Q_u} + \frac{1}{Q_e} \tag{6}$$

where Q_u is the self or internal (unloaded) quality factor of the CPWR without being coupled to the through-line. Theoretically, a lossless CPWR has infinite unloaded Q-factor, $Q_u = \infty$. However, practically, Q_u is limited by the conductor and dielectric losses, which is discussed later on. It should be noted that, for low-loss CPWR, the external Q-factor Q_e dominates the total Q-factor expressed by Eq. (6).

The external Q-factor can be expressed as follows.

$$\frac{1}{Q_e} = \frac{1}{Q_R} + \frac{1}{Q_C} \tag{7}$$

where Q_R is an equivalent Q-factor related to the radiation loss, and Q_C is an equivalent Q-factor related to the reactive coupling between the resonator and the through-line, which can be considered as a loss channel.

3.2. Calculating the Unloaded Quality Factor of the CPWR

For the bandstop filter design shown in Figure 1, the CPW region forming the perimeter of the U-shape can be considered an open-ended half-wavelength transmission line resonator. The unloaded Q-factor of both short-circuited and open-circuited half-wavelength CPWR can be expressed as follows [28],

$$Q_u = \frac{\pi}{2\alpha L_{R_{1/2}}} = \frac{\beta_0}{2\alpha}\sqrt{\varepsilon}_{r_{eff}} = \frac{\omega_0}{2c\alpha}\sqrt{\varepsilon}_{r_{eff}} \tag{8}$$

where $L_{R_{1/2}}$ is the length of the half-wavelength resonator, β_0 the free space wave number, ω_0 the resonant angular frequency, α the attenuation constant of the CPW, and $\varepsilon_{r_{eff}}$ is given by Eq. (2).

The attenuation constant α of the CPW is related by the conductor and dielectric losses, and hence, it can be expressed as follows.

$$\alpha = \alpha_c + \alpha_d \tag{9}$$

where α_c is the attenuation caused by the conductor loss whereas α_d is the attenuation caused by the dielectric substrate loss. For a transmission line made of high-conductivity metals like copper ($\sigma = 5.6 \times 10^7$ S/m), the dielectric loss dominates, which means that $\alpha_d \gg \alpha_c$, and hence, for a CPW carrying TEM mode, the attenuation constant can be approximated as follows.

$$\alpha \approx \alpha_d = \frac{\omega_0 \tan\delta}{2c}\sqrt{\varepsilon}_{r_{eff}} \tag{10}$$

Making use of Eq. (10), Eq. (8) of the unloaded Q-factor of the CPWR is reduced to the following.

$$Q_u \approx \frac{1}{\tan\delta} \tag{11}$$

Substituting from Eq. (11) into Eq. (6), the total quality factor can be expressed as

$$Q \approx \frac{Q_e}{1 + Q_e \tan\delta} \tag{12}$$

The last expression can be used to calculate the external Q-factor, Q_e, if the loss tangent of the dielectric substrate is known given that Q has been obtained by simulation.

3.3. Semi-Analytical Method for Calculating the Coupling *Q*-Factor

Semi-analytic techniques are used to solve electromagnetic problems giving some physical insight of the underlying principles [29–32]. It may be useful to assess the effect of the reactive load caused by broadside-coupling to the CPWTL on the Q-factor of the U-shaped CPWR. This can be achieved by evaluating Q_C which is related to reactive coupling. As this Q-factor is difficult to be evaluated analytically, a semi-analytic method is proposed in the present section. First, the total Q-factor, Q, of the bandstop filter is obtained numerically by electromagnetic simulation, where the commercially available CST$^{\text{TM}}$ package is used in the present work for this purpose. A low profile of the CPW ensures low radiation loss, and hence, the term $1/Q_R$ in Eq. (7) can be neglected leading to the following expression for the external Q-factor.

$$Q_e \approx Q_C \tag{13}$$

The last expression means that the external Q-factor is dominated by the coupling Q-factor for a well-designed bandstop filter. Making use of Eqs. (12) and (13), the coupling Q-factor can be evaluated as follows.

$$Q_c \approx \frac{Q}{1 - Q\delta} \tag{14}$$

4. NUMERICAL RESULTS AND EXPERIMENTAL MEASUREMENTS

In the present section, both the numerical results obtained by simulation and the experimental results obtained by microwave measurements of the fabricated bandstop filter prototype are presented, discussed, and compared for the purpose of arriving at accurate performance assessment and understanding of the resonance mechanism underlying the proposed bandstop filter operation. Also, the results for the external Q-factor obtained by the semi-analytic method described in Subsection 3.3 are presented and discussed. It should be noted that the following presentations and discussions of numerical and experimental results are concerned with bandstop filter as that shown in Figure 1 designed with the following dimensional parameters, unless otherwise stated: $s = 0.1$ mm, $w = 0.1$ mm, $w_G = 0.2$ mm, $L_B = 10$ mm, $W_b = 8.6$ mm, $L_A = 26.2$ mm and $L_T = 25.2$ mm, $L_R = 2L_A + L_B$. The substrate material is Rogers RO4003C$^{\text{TM}}$ with dielectric constant $\varepsilon_r = 3.38$, dielectric loss tangent $\tan\delta = 0.0021$, and height $h = 0.4$ mm. The metal strips and ground are made of copper and have conductivity $\sigma = 5.6 \times 10^7$ S/m. A model with the same dimensions as that of the experimental prototype of the bandstop filter is constructed for electromagnetic simulation using the commercially available CST$^{\text{TM}}$

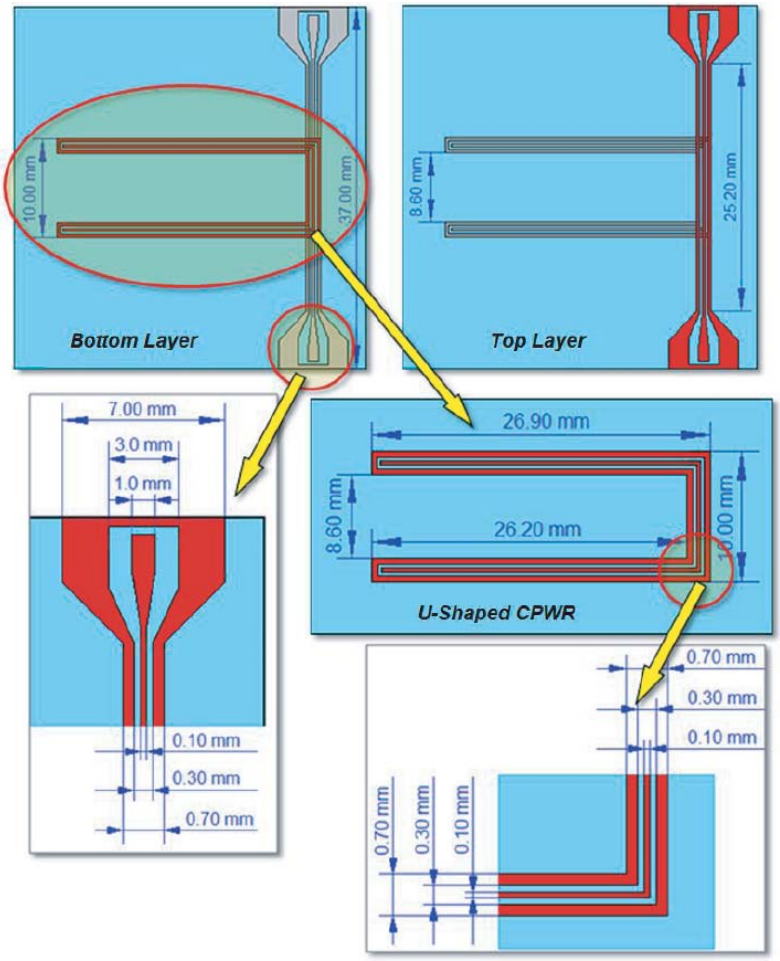

Figure 2. Dimensions for the CST^{TM} model of the proposed bandstop filter (Note: the red color is for the strips printed on the viewed layer whereas the gray color is for the strips printed on the other layer).

package. This model is presented in Figure 2 showing the detailed dimensions. At input and output ports of the proposed filter, the transitional tapered CPW region is designed to satisfy impedance matching between the 50 Ω impedance of the microwave source and the characteristic impedance of the CPWTL.

In the following presentation, some comparisons are made between the simulated and experimental results concerned with the frequency response of the bandstop filter at its 1st and 2nd resonances.

4.1. Frequency Response of Bandstop Filter

The frequency response of the transmission coefficients $|S_{21}|$ of the proposed dual bandstop filter having the design parameters given in the introduction of Section 4 is presented in Figure 3. It is assumed that the CPWR is made of copper conductors on a dielectric substrate of $\varepsilon_r = 4.5$ and loss tangent $\delta = 0.002$. The frequency response exhibits two sharp anti-peaks: the first one is at $f = 1.576$ GHz, with Q-factor of 140, whereas the second anti-peak is at $f = 3.15$ GHz, with Q-factor of 16.

The mechanisms leading to these values of the resonant frequencies and the corresponding Q-factors can be explained in view of the surface current distributions at the 1st- and 2nd-order resonance frequencies of the open ended CPWR formed by the perimeter of the U-shape, which are presented in Figures 4(a) and 4(b), respectively. At the 1st-order resonance, the current distribution has one maximum value at the center of the base of the U-shape, whereas the current distribution shows two

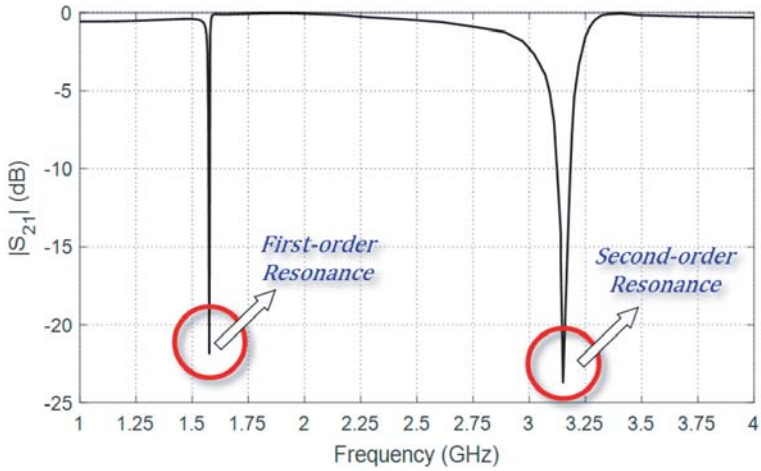

Figure 3. Frequency response of the transmission coefficient $|S_{21}|$ of the bandstop filter (with the design shown in Figure 2) based on the U-shaped half-wave length CPWR.

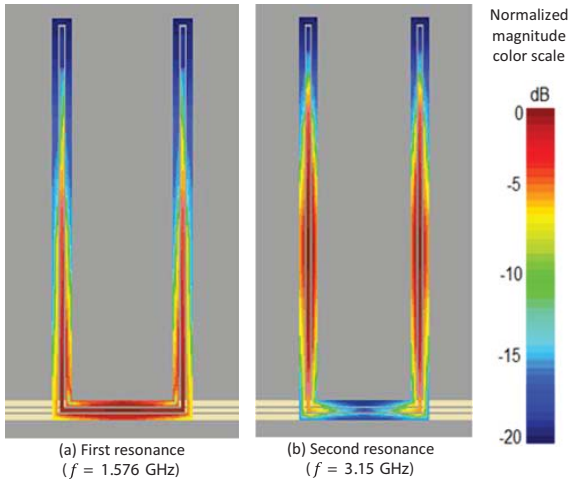

Figure 4. Surface current on the conductors at the frequencies corresponding to the 1st-order and 2nd-order resonances of the U-shaped CPWR.

maxima near the centers of the arms of the U-shape.

It is shown that as this CPW region is a half-wavelength resonator whose total length is 62.4 mm, the resonance frequencies can be calculated using Eq. (1), which gives $f_1 = 1.61$ GHz and $f_2 = 3.22$ GHz. The slight deviation of the resonant frequencies obtained by simulation from the theoretical values obtained using Eq. (1) can be attributed to the reactive load resulting from coupling the CPWTL to the CPWR because part of the energy is stored in the electric field of the coupling capacitance and thereby causing a shift of the resonant frequency. Moreover, a part of the frequency shift can be attributed to the error of the approximate analytic formula for $\varepsilon_{r_{eff}}$ given by Eq. (2).

4.1.1. Tuning the Center Frequency of the Bandstop Filter

As given in Table 1, the main design parameter to tune the center frequency of the bandstop filter according to Eq. (1) is the total length of the U-shaped CPWR, L_R. Figure 5 shows the change of the frequency response of the transmission coefficient $|S_{21}|$ of the bandstop filter around the 1st resonance frequency with changing the resonator length, L_R, while keeping the coupling length L_B constant. It is

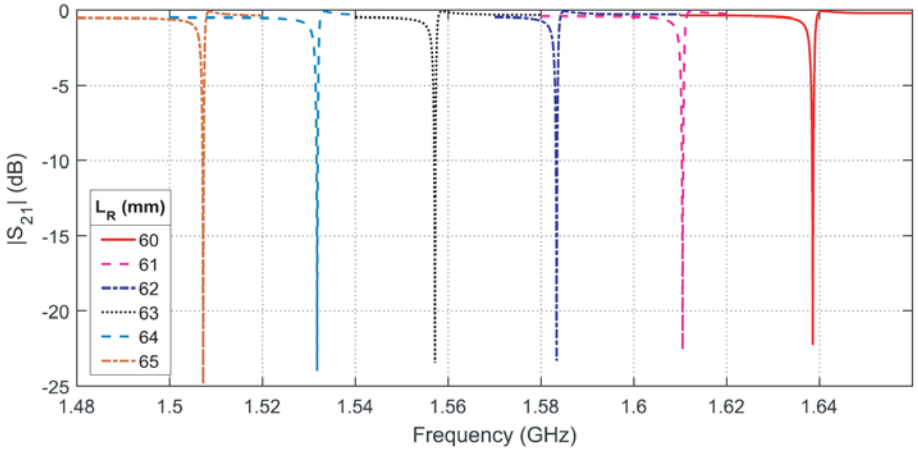

Figure 5. Change of the frequency response of the transmission coefficient $|S_{21}|$ of the bandstop filter around the 1stresonance frequency with changing the CPWR length, L_R.

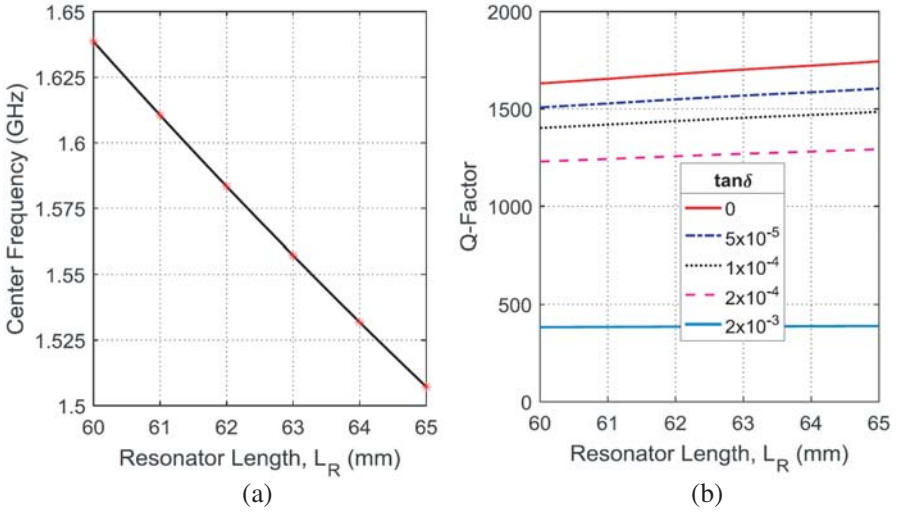

Figure 6. Dependence of the center frequency and the Q-factor of the bandstop filter on the resonator length at the 1st resonance frequency of the U-shaped CPWR. (a) Dependence of the center frequency on the CPWR length ($\tan\delta = 0$). (b) Dependence of the Q-factor on the CPWR length for different values of $\tan\delta$.

clear that the resonance frequency decreases with increasing the resonator length L_R which agrees with the analytical formula given by Eq. (1). This is clear in Figure 6(a) which shows that the resonance frequency is inversely proportional to L_R. However, as shown in Figure 6(b), the Q-factor is almost independent of the resonator length L_R as long as the coupling length L_B is constant.

4.1.2. Adjusting the Q-Factor of the Bandstop Filter

As previously discussed, the Q-factor of the bandstop filter is dominated by the external Q-factor which is attributed mainly to the broadside coupling between the CPWR and CPWTL. The coupling strength is strongly dependent on the length of the CPW regions over which the coupling is performed. Consequently, the length of the base of the U-shape, L_B, is an important design parameter that controls the Q-factor at each resonance frequency. Figure 7 shows the change of the frequency response of the transmission coefficient $|S_{21}|$ of the bandstop filter around the 1st resonance frequency with changing

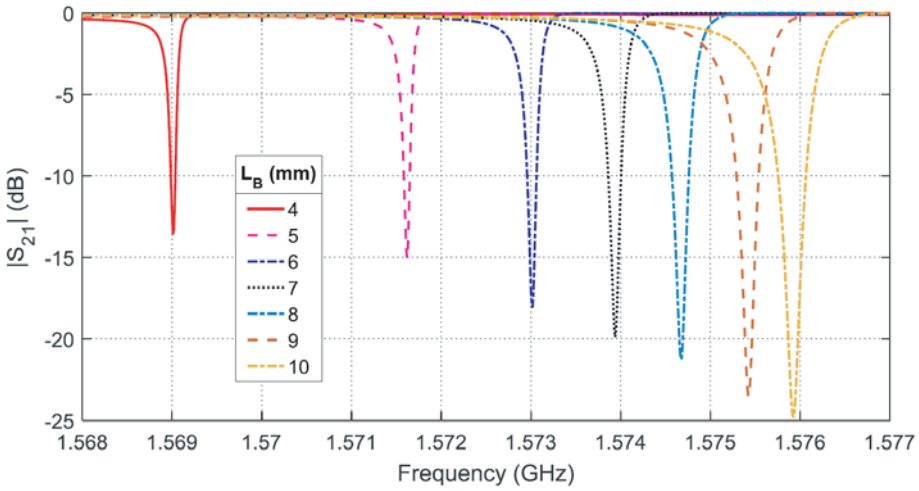

Figure 7. Change of the frequency response of the transmission coefficient $|S_{21}|$ of the bandstop filter around the 1st resonance frequency with changing the coupling length, L_B while keeping the CPWR length, L_R constant.

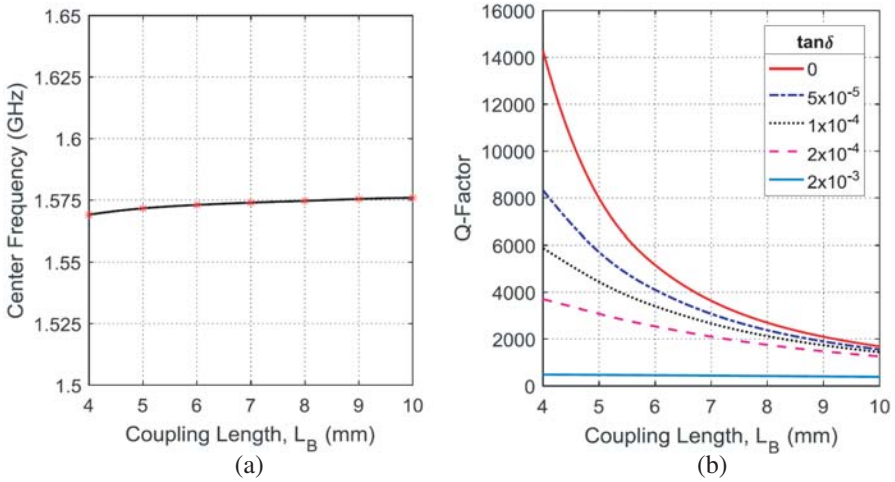

Figure 8. Dependence of the Q-factor and center frequency of the bandstop filteron the coupling length at the 1st resonance frequency of the U-shaped CPWR. (a) Dependence of the center frequency on the coupling length ($\tan\delta = 0$). (b) Dependence of the Q-factor on the coupling length for different values of $\tan\delta$.

the coupling length, L_B, between the CPWR and CPWTL while keeping the total length of the CPWR constant. It is clear that the resonance frequency slightly increases with increasing L_B due to the change of the reactive load impedance equivalent to the broadside coupling. However, Figure 8(a) shows that the center frequency is almost independent of L_B as long as the total resonator length L_R is constant. The Q-factor is considerably decreased with increasing the coupling length as shown in Figure 8(b). As the coupling length increases the reactive load caused by the broadside coupling increases leading to a decrease of the external Q-factor which, in turn, results in considerable decrease of the total Q-factor.

The strength of broadside coupling is strongly dependent on the separation distance between the two coupled lines. Consequently, the height of the dielectric substrate, h, is an important design parameter that controls the Q-factor at each resonance frequency. Figure 9 shows the change of the frequency response of the transmission coefficient $|S_{21}|$ of the bandstop filter around the 1st resonance frequency with changing the substrate height. It is clear that the resonance frequency slightly decreases with

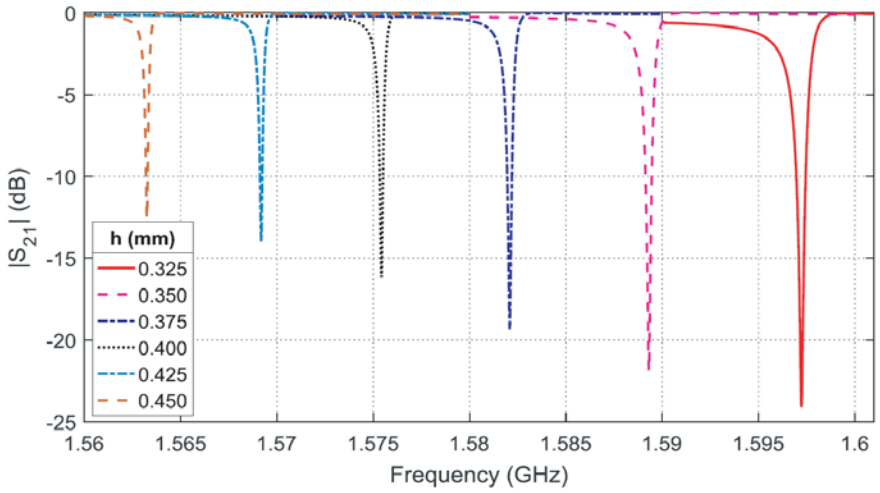

Figure 9. Change of the frequency response of the transmission coefficient $|S_{21}|$ of the bandstop filter around the 1st resonance frequency with changing the substrate height, h.

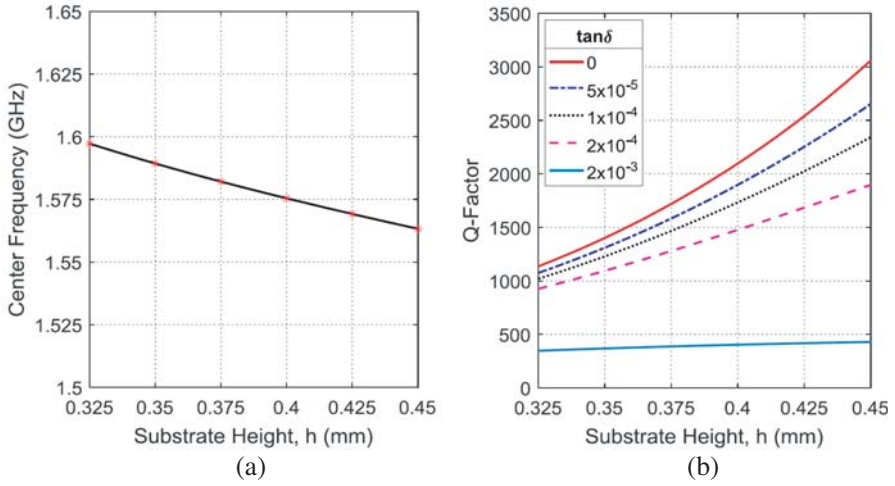

Figure 10. Dependence of the Q-factor and center frequency of the bandstop filter on the substrate height at the 1st resonance frequency of the U-shaped CPWR. (a) Dependence of the center frequency on the substrate height ($\tan\delta = 0$). (b) Dependence of the Q-factor on the substrate height for different values of $\tan\delta$.

increasing h due to the change of the reactive load impedance equivalent to the broadside coupling. Figure 10(a) shows that the center frequency is slightly dependent on h. The Q-factor is considerably increased with increasing the substrate height as shown in Figure 10(b). As the substrate height decreases the reactive load caused by the broadside coupling increases leading to a decrease of the external Q-factor which, in turn, results in considerable decrease of the total Q-factor.

4.1.3. Frequency Response of the Bandstop Filter at Higher-Order Resonances

It may be interesting to study the characteristics of the bandstop filter at a higher-order resonance by studying the frequency response of the transmission coefficient $|S_{21}|$ around this resonance. The 3rd-order resonance of the proposed bandstop filter whose dimensions are given at the beginning of Section 4 is taken a case-study for this purpose.

Figure 11 shows the change of the frequency response of the transmission coefficient $|S_{21}|$ of the

bandstop filter around the 3rd resonance frequency with changing the coupling length, L_B, between the CPWR and CPWTL while keeping the total length of the CPWR constant. It is clear that the resonance frequency slightly increases with increasing L_B due to the change of the reactive load impedance equivalent to the broadside coupling. However, Figure 12(a) shows that the center frequency is almost independent of L_B as long as the total resonator length L_R is constant. The Q-factor is strongly dependent on the coupling length as shown in Figure 12(b). As the coupling length increases the reactive load caused by the broadside coupling increases leading to a considerable decrease of the total Q-factor.

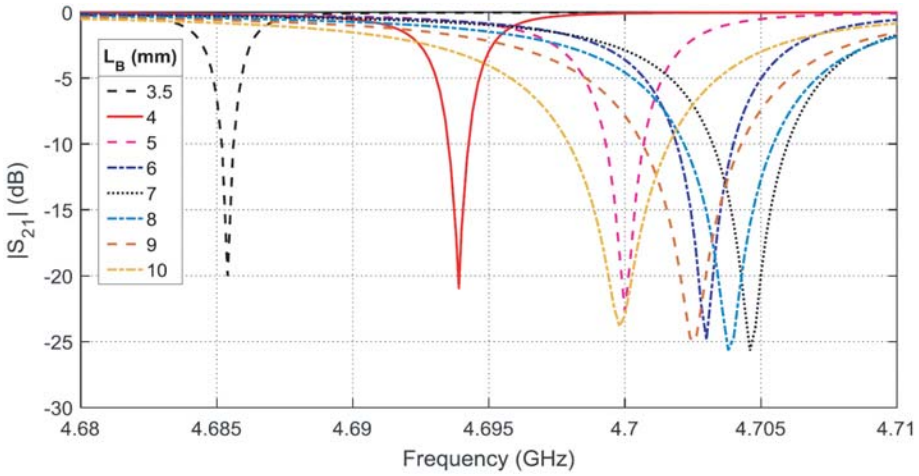

Figure 11. Change of the frequency response of the transmission coefficient $|S_{21}|$ of the bandstop filter around the 3rd-order resonance frequency with changing the coupling length, L_B, while keeping the CPWR length, L_R constant.

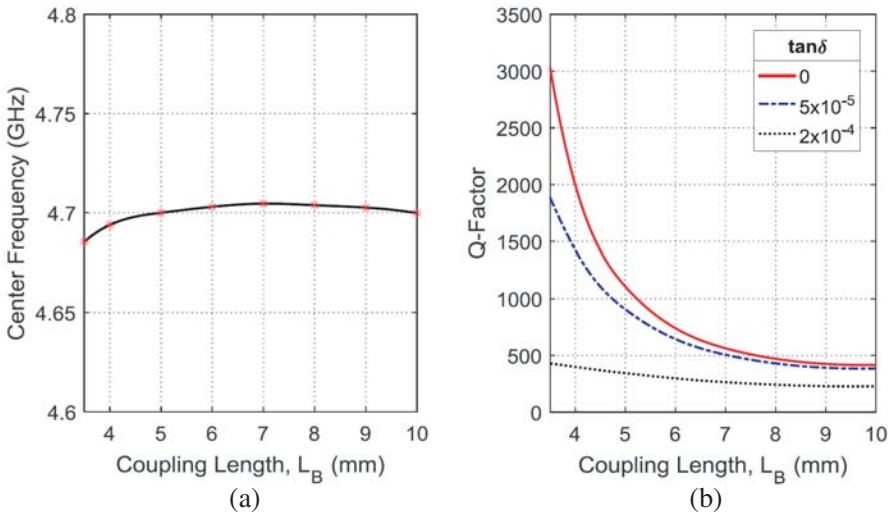

Figure 12. Dependence of the Q-factor and center frequency of the bandstop filter on the coupling length at the 3rd-order resonance frequency of the U-shaped CPWR. (a) Dependence of the center frequency on the coupling length L_B, ($\tan\delta = 0$). (b) Dependence of the Q-factor on the coupling length L_B, for different values of $\tan\delta$.

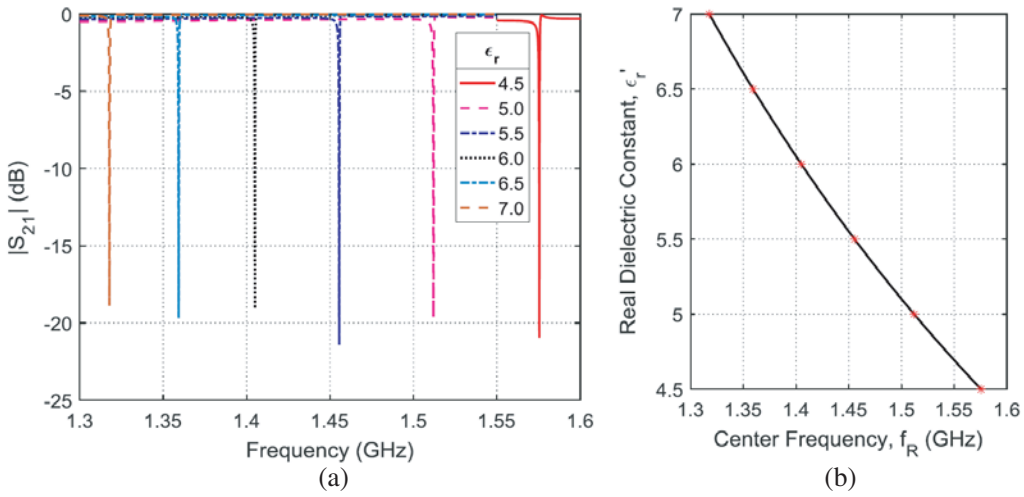

Figure 13. High selectivity of the proposed bandstop filter demonstrates strong dependence of the 1st resonance frequency on the dielectric constant of the substrate material. (a) Change of the frequency response of the transmission coefficient $|S_{21}|$ of the bandstop filter around the 1st resonance frequency with changing the dielectric constant of the substrate. (b) Dependence of the real part of the dielectric constant of the substrate on the center frequency ($\tan\delta = 0$).

4.1.4. Using the Proposed Bandstop Filter as a Dielectric Sensor

The dielectric tensor can be measured using highly selective devices like those proposed in [33–36]. However, as the dispersive and anisotropic materials are beyond the scope of the present study, this section is concerned with demonstrating the validity of such an application by, simply, studying the sensitivity of the resonant frequency of the filter on the complex dielectric constant of the substrate material. It is shown that the bandstop filter (of the proposed design dimensions) can be used as a dielectric sensor just in monitoring the real and imaginary parts of the dielectric constant of the substrate material by measuring the resonance frequency and Q-factor. Figure 13(a) shows the change of the frequency response of the transfer function with changing the dielectric constant of the substrate. The real part of the dielectric constant can be estimated using the relation plotted in Figure 13(b). As shown in Figure 14, the imaginary part of the dielectric constant is strongly dependent on both the resonant frequency and Q-factor. Thus, the curves plotted in Figures 14(a), (b) in addition to that plotted in Figure 13(b) can be used to estimate the complex dielectric constant of the substrate material.

4.1.5. Procedure for the Optimal Design Parameters of the Bandstop Filter

The design goals of the bandstop filter design are the impedance matching at the two filter ports and the target values of the resonance frequency and the rejection bandwidth or, equivalently, the Q-factor. The procedure followed to get the optimal parameters for the bandstop filter design that achieves the required goals can be explained more thoroughly as follows.

(i) Using Equation (5), impedance matching at the filter ports can be achieved by setting the values of the strip and slot widths, w and s, respectively so as to get $Z_0 = 50\,\Omega$.

(ii) Using the curve presented in Figure 6(a), the required resonance frequency, f_R, is satisfied by setting the resonator length, L_R, to the value corresponding to f_R value while keeping the coupling length L_B constant.

(iii) Using the curve presented in Figure 8(b), the required Q-factor (equivalently, the bandwidth) can be achieved by setting the coupling length (base of the U-shape), L_B, to the value corresponding to the required Q-value while keeping the total resonator length L_R constant.

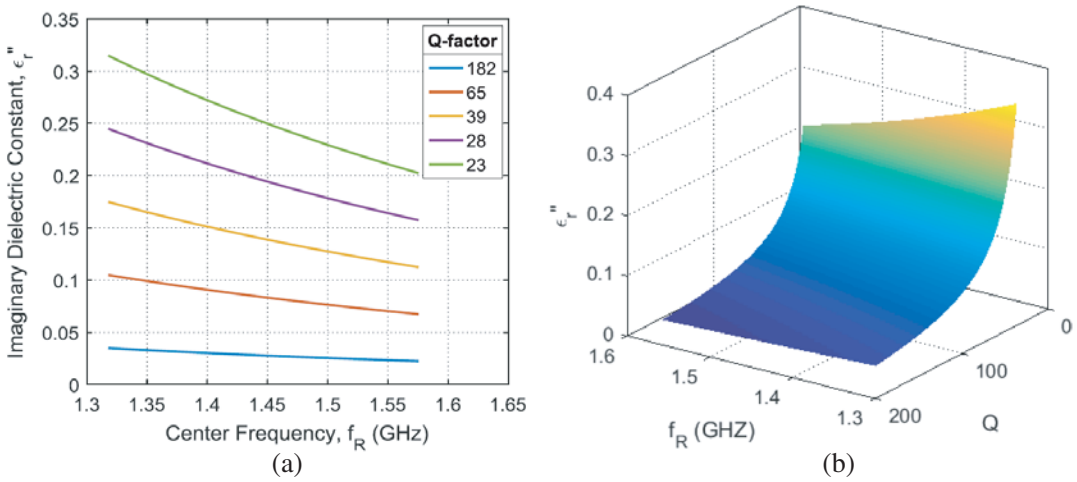

Figure 14. Assessment of the complex dielectric constant of the substrate material by measuring the resonant frequency and the Q-factor of the bandstop filter. (a) Dependence of the imaginary part of the dielectric constant of the substrate on the center frequency for different values of the Q-factor. (b) Dependence of the imaginary part of the dielectric constant of the substrate on the center frequency and the Q-factor.

(iv) An alternative way to achieve the required Q-factor or bandwidth is to use the curve presented in Figure 9(b) to set the substrate height, h, to the value corresponding to the required Q-value.

4.2. Experimental Assessment of the Bandstop Filter

The purpose of the experimental work is to study the underlying physical principles of operation and to investigate the performance of the proposed high Q-factor bandstop filter based on broadside coupling between U-shaped CPWR and CPWTL.

4.2.1. Prototype Fabrication

A prototype of the proposed bandstop filter is fabricated for experimental studying of the underlying physical principles of operation and investigating the filter performance. The dimensional parameters of the fabricated filter are those presented in Figure 2. The substrate used for fabrication is RO4003C$^{\text{TM}}$, with substrate height $h = 0.4\,\text{mm}$, dielectric constant $\varepsilon_r = 3.38$, and dielectric loss tangent $\tan\delta = 0.0021$. The same design dimensions given at the beginning of Section 4 are used for fabrication. A photograph of the fabricated prototypes is presented in Figure 15, where its size is compared to a metal coin of the standard one-inch diameter.

4.2.2. Experimental Setup

The vector network analyzer (VNA) of the Keysight (Agilent) FieldFox N9928A$^{\text{TM}}$ is used to measure the transmission and reflection coefficients $|S_{21}|$ and $|S_{11}|$, respectively, of the bandstop filter prototype under test. For this purpose the filter prototype is mounted on the substrate test fixture as shown in Figure 16(a). After performing the required settings and calibration procedure, the test fixture holding the prototype under test is connected to the VNA as shown in Figure 16(b).

4.2.3. Experimental Results

The frequency responses of the transmission and reflection coefficients $|S_{21}|$ and $|S_{11}|$ of this filter over the frequency bands around the 1$^{\text{st}}$ and 2$^{\text{nd}}$ resonances are presented in Figures 17 and 18, respectively. The measurements are achieved by the VNA and compared to that obtained by simulation using the

Figure 15. The fabricated prototype of the proposed high Q-factor bandstop filter.

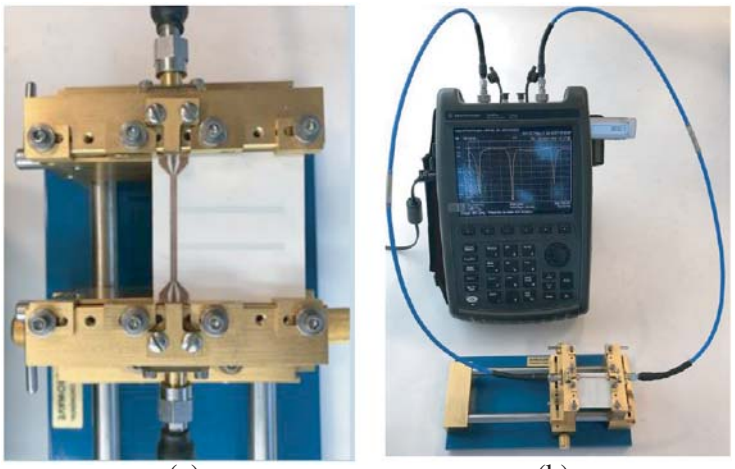

(a) (b)

Figure 16. Measurement of the frequency response of the fabricated prototype for experimental investigation of the proposed bandstop filter. (a) The fabricated bandstop filter mounted on the VNA test fixture. (b) Measurement of the transmission coefficient $|S_{21}|$ using the VNA.

commercially available CST^{TM} software package. It is clear that the experimental measurements and simulation results show good agreement.

The experimental measurements of the frequency response at the lower band of the bandstop filter show that the 1st resonance occurs at $f_{1^{st}}^{(Exp)} = 1.578\,GHz$, whereas the simulation results show that this resonance occurs at $f_{1^{st}}^{(Sim)} = 1.576\,GHz$. The corresponding Q-factors are $Q_{1^{st}}^{(Exp)} = 131$ and $Q_{1^{st}}^{(Sim)} = 140$. The external Q-factor which is dominated by the coupling Q-factor as discussed before can be obtained by a semi-analytic approach as described in Subsection 3.3. The unloaded Q-factor can be calculated in terms of the dielectric substrate loss tangent using Eq. (11) to get $Q_u = 476$. The external Q-factor, which is dominantly attributed to broadside coupling, can be obtained by Eqs. (6) and (12) to get $Q_{e1^{st}}^{(Exp)} = 181$ using the measurement data and $Q_{e1^{st}}^{(Sim)} = 200$ using simulation data, where subscript "1st" indicates the 1st resonance. Such a high value of the external Q-factor can be attributed to the strong broadside coupling between the CPWR and CPWTL.

Similarly, the experimental measurements and simulation give the following results for upper stop band at the 2nd resonance of the U-shaped CPWR: $f_{2^{nd}}^{(Exp)} = 3.169\,GHz$, $f_{2^{nd}}^{(Sim)} = 3.15\,GHz$, $Q_{2^{nd}}^{(Exp)} = 16$

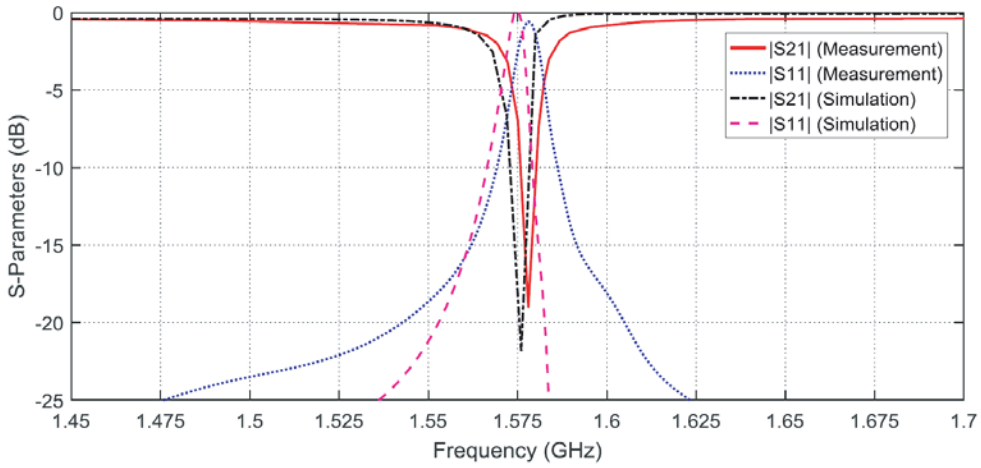

Figure 17. Frequency responses of the transmission and reflection coefficients $|S_{21}|$ and $|S_{11}|$, respectively, of the bandstop filter at the 1st resonance of the half-wave U-shaped CPWR which is broadside-coupled to the CPWTL.

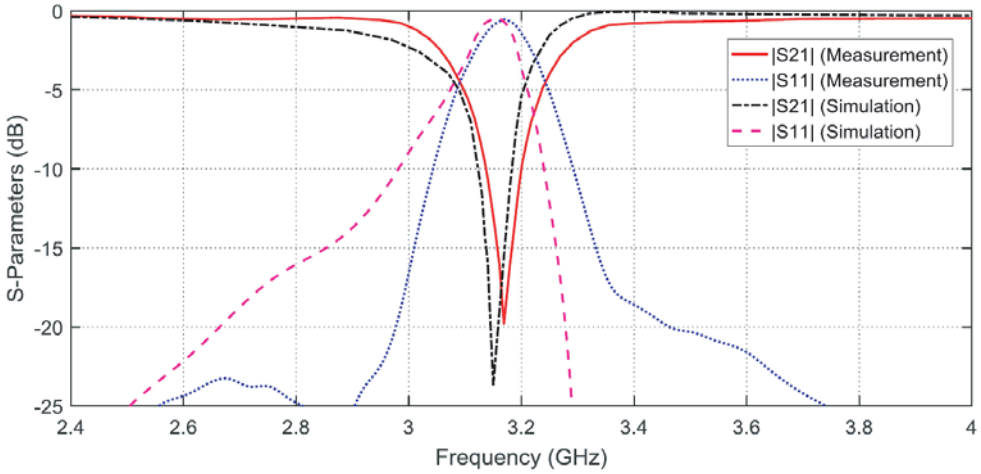

Figure 18. Frequency responses of the transmission and reflection coefficients $|S_{21}|$ and $|S_{11}|$, respectively, of the bandstop filter at the 2nd resonance of the half-wave U-shaped CPWR which is broadside-coupled to the CPWTL.

Table 2. Comparison between Q-factors of bandstop filters achieved experimentally in other published work compared with that achieved in the present work.

Published Work	Huang et al. [24]	Woo et al. [23]	Liu et al. [26]	Lee et al. [25]	Kakhki et al. [25]	Present Work
Q-factor	31.67	36.05	45	49.7	57	131

and $Q_{2^{\text{nd}}}^{(\text{Sim})} = 17$. Accordingly, the obtained values of the external Q-factor are $Q_{e2^{\text{nd}}}^{(\text{Exp})} = 16.5$ and $Q_{e2^{\text{nd}}}^{(\text{Sim})} = 17.5$. In comparison to the Q-factor of the bandstop filter obtained at the 2nd resonance, the Q-factor obtained at the 1st resonance is much higher, which indicates that the broadside coupling at 1st resonance of the CPWR is much more efficient as it results in much lower loss than that caused by broadside coupling at the 2nd order resonance.

Comparisons among the Q-factors of some bandstop filters achieved experimentally in other published work compared with that achieved in the present work are listed in Table 2. The higher value of the Q-factor achieved in the present work is due to the strong broadside coupling and optimized dimensions of the U-shaped CPWR mainly the coupling length L_c which is the length of the U-shape base.

5. CONCLUSION

The design of a high Q-factor bandstop filter based on broadside-coupling between U-shaped CPWR and CPWTL is presented. The CPWTL is printed on one layer of relatively thin dielectric substrate whereas the CPWR is printed on the opposite layer. The proposed bandstop filter is shown to have much higher Q-factor than other published work. Such a high Q-factor is attributed to the finite width of the side ground strips. Due to the lower profile of the CPW with finite-width, the radiation loss is reduced leading to enhanced Q-factor. The dimensions of the CPWTL are optimized for impedance matching whereas the dimensions of the U-shaped CPWR are optimized to obtain the highest possible Q-factor. The numerical results concerned with the effect of the loss tangent of the dielectric substrate material on the Q-factor are presented and discussed. A prototype of the proposed filter is fabricated and experimentally studied where the measurements show good agreement compared with the corresponding simulation results.

REFERENCES

1. Eldesouki, E., K. F. A. Hussein, and A. M. El-Nadi, "Circularly polarized arrays of cavity backed slot antennas for X-band satellite communications," *Progress In Electromagnetics Research B*, Vol. 9, 179–198, 2008.
2. Hussein, K. F. A., "Effect of internal resonance on the radar cross section and shield effectiveness of open spherical enclosures," *Progress In Electromagnetics Research*, Vol. 70, 225–246, 2007.
3. Göppl, M., A. Fragner, M.Baur, R. Bianchetti, S. Filipp, J. M. Fink, P. J. Leek, G. Puebla, L. Steffen, and A. Wallraff, "Coplanar waveguide resonators for circuit quantum electrodynamics," *Journal of Applied Physics*, Vol. 104, No. 11, 113904, 2008.
4. Li, H. J., Y. W. Wang, L. F. Wei, P. J. Zhou, Q. Wei, C. H. Cao, Y. R. Fang, Y. Yu, and P. H. Wu, "Experimental demonstrations of high-Q superconducting coplanar waveguide resonators," *Chinese Science Bulletin*, Vol. 58, No. 20, 2413–2417, 2013.
5. Liu, G., Z.-Y. Wang, J.-J. Wu, and L. Li, "Capacitive loaded U-slot defected ground structure for bandstop filter with improvement Q factor," *Progress In Electromagnetics Research Letters*, Vol. 65, 31–36, 2017.
6. Lai, Y.-L. and P.-Y. Cheng, "CPW filters with defected ground structures for RF and microwave applications," *9th Joint International Conference on Information Sciences (JCIS-06)*, Atlantis Press, 2006.
7. Deng, P.-H., C.-H. Wang, and C. H. Chen, "Novel broadside-coupled bandpass filters using both microstrip and coplanar-waveguide resonators," *IEEE Transactions on Microwave Theory and Techniques*, Vol. 54, No. 10, 3746–3750, 2006.
8. Lee, S., S. Oh, W.-S. Yoon, and J. Lee, "A CPW bandstop filter using double hairpin-shaped defected ground structures with a high Q factor," *Microwave and Optical Technology Letters*, Vol. 58, No. 6, 1265–1268, 2016.
9. Kumar, A., A. K. Verma, and Q. Zhang, "Compact triple-band bandstop filters using embedded capacitors," *Progress In Electromagnetics Research Letters*, Vol. 63, 15–21, 2016.
10. Yang, S., Z. Xiao, and S. Budak, "Design of triband bandstop filter using an asymmetrical cross-shaped microstrip resonator," *Progress In Electromagnetics Research Letters*, Vol. 86, 35–42, 2019.
11. Hammed, R. T. and B. H. Hameed, "Compact multiple bandstop filter using integrated circuit of defected microstrip structure (DMS) and dual-mode resonator," *AEU-International Journal of Electronics and Communications*, Vol. 107, 209–214, 2019.

12. Yan, J.-M., L. Cao, and H.-Y. Zhou, "A novel quad-band bandstop filter based on coupled-line and shorted stub-loaded half-wavelength microstrip resonator," *Progress In Electromagnetics Research Letters*, Vol. 79, 65–70, 2018.
13. Abu Safia, O., A. A. Omar, and M. C. Scardelletti, "Design of dual-band bandstop coplanar waveguide filter using uniplanar series-connected resonators," *Progress In Electromagnetics Research Letters*, Vol. 27, 93–99, 2011.
14. Ning, H., J. Wang, Q. Xiong, and L.-F. Mao, "Design of planar dual and triple narrow-band bandstop filters with independently controlled stopbands and improved spurious response," *Progress In Electromagnetics Research*, Vol. 131, 259–274, 2012.
15. Min, X.-L. and H. Zhang, "Design of dual-band bandstop filter based on dumbbell-shaped resonators and U-shaped slot," *Progress In Electromagnetics Research Letters*, Vol. 71, 133–140, 2017.
16. Everard, J. K. A. and K. K. M. Cheng, "High performance direct coupled bandpass filters on coplanar waveguide," *IEEE Transactions on Microwave Theory and Techniques*, Vol. 41, No. 9, 1568–1573, 1993.
17. Sghir, E., A. Errkik, J. Zbitou, A. Tajmouati, and M. Latrach, "A novel compact CPW band-stop filter using O-DGS configuration," *International Journal of Electrical & Computer Engineering*, Vol. 9, 2088–8708, 2019.
18. Contreras, A., M. Ribó, L. Pradell, V. Raynal, I. Moreno, M. Combes, and M. Ten, "Compact fully uniplanar bandstop filter based on slow-wave multimodal CPW resonators," *IEEE Microwave and Wireless Components Letters*, Vol. 28, No. 9, 780–782, 2018.
19. Gupta, K. C., R. Garg, and I. Bahl, *Microstrip Lines and Slotlines*, Artech, Dedham, MA, 1979.
20. Gopinath, A., "Losses in coplanar waveguides," *IEEE Transactions on Microwave Theory and Techniques*, Vol. 30, No. 7, 1101–1104, 1982.
21. Williams, F. D. and S. E. Schwarz, "Design and performance of coplanar waveguide bandpass filters," *IEEE Transactions on Microwave Theory and Techniques*, Vol. 31, No. 7, 558–566, 1983.
22. Woo, D. J., T. K. Lee, J. W. Lee, C. S. Pyo, and W. K. Choi, "Novel U-slot and V-slot DGSs for bandstop filter with improved Q factor," *IEEE Transactions on Microwave Theory and Techniques*, Vol. 54, No. 6, 2840–2847, 2006.
23. Huang, S. Y. and Y. H. Lee, "A compact E-shaped patterned ground structure and its applications to tunable bandstop resonator," *IEEE Transactions on Microwave Theory and Techniques*, Vol. 57, No. 3, 657–666, 2009.
24. Kakhki, M. A. and M. H. Neshati, "Numerical investigation and experimental study of two novel band-reject DGS filters with a very high Q-factor," *19th Iranian Conference on Electrical Engineering*, 1–4, IEEE, 2011.
25. Lee, S., S. Oh, W. S. Yoon, and J. Lee, "A CPW bandstop filter using double hairpin-shaped defected ground structures with a high Q factor," *Microwave and Optical Technology Letters*, Vol. 58, No. 6, 1265–1268, 2016.
26. Kumar, M. and R. Gowri, "Review on various issues and design topologies of edge coupled coplanar waveguide filters," *Journal of Graphic Era University*, Vol. 5, No. 2, 91–96, 2017.
27. Simons, R. N., *Coplanar Waveguide Circuits, Components, and Systems*, Vol. 165, John Wiley & Sons, 2004.
28. Pozar, D. M., *Microwave Engineering*, John Wiley & Sons, Inc., 2012.
29. Valagiannopoulos, C. A. and N. L. Tsitsas, "On the resonance and radiation characteristics of multi-layered spherical microstrip antennas," *Electromagnetics*, Vol. 28, No. 4, 243–264, 2008.
30. Alitalo, P., C. A. Valagiannopoulos, and S. A. Tretyakov, "Simple cloak for antenna blockage reduction," *2011 IEEE International Symposium on Antennas and Propagation (APSURSI)*, 669–672, IEEE, 2011.
31. Chen, L., X. Ren, Y.-Z. Yin, and Z. Wang, "Broadband CPW-fed circularly polarized antenna with an irregular slot for 2.45 GHz RFID reader," *Progress In Electromagnetics Research Letters*, Vol. 41, 77–86, 2013.

32. Valagiannopoulos, C. A., "Semi-analytic solution to a cylindrical microstrip with inhomogeneous substrate," *Electromagnetics*, Vol. 27, No. 8, 527–544, 2007.
33. Valagiannopoulos, C. A., "On measuring the permittivity tensor of an anisotropic material from the transmission coefficients," *Progress In Electromagnetics Research B*, Vol. 9, 105–116, 2008.
34. Zhou, T., T. Hu, and Z. Ge, "Dispersive Rayleigh wave attenuation using inverse-dispersion method," *ASEG Extended Abstracts*, Vol. 2010, No. 1, 1–4, 2010.
35. Tagay, Z. and C. Valagiannopoulos, "Highly selective transmission and absorption from metasurfaces of periodically corrugated cylindrical particles," *Physical Review B*, Vol. 98, No. 11, 115306, 2018.
36. Siddiqui, O. F. and A. S. Mohra, "Microwave dielectric sensing in hyperbolically dispersive media," *IEEE Sensors Letters*, Vol. 1, No. 6, 1–4, 2017.